

Figure S1. The schematic illustration of the soil sampling design. Sampling of soil was performed under an individual fruitbody (**A**) or two fruitbodies of different species, located next to each other (**B**). Each subsample represents one core drill dig.

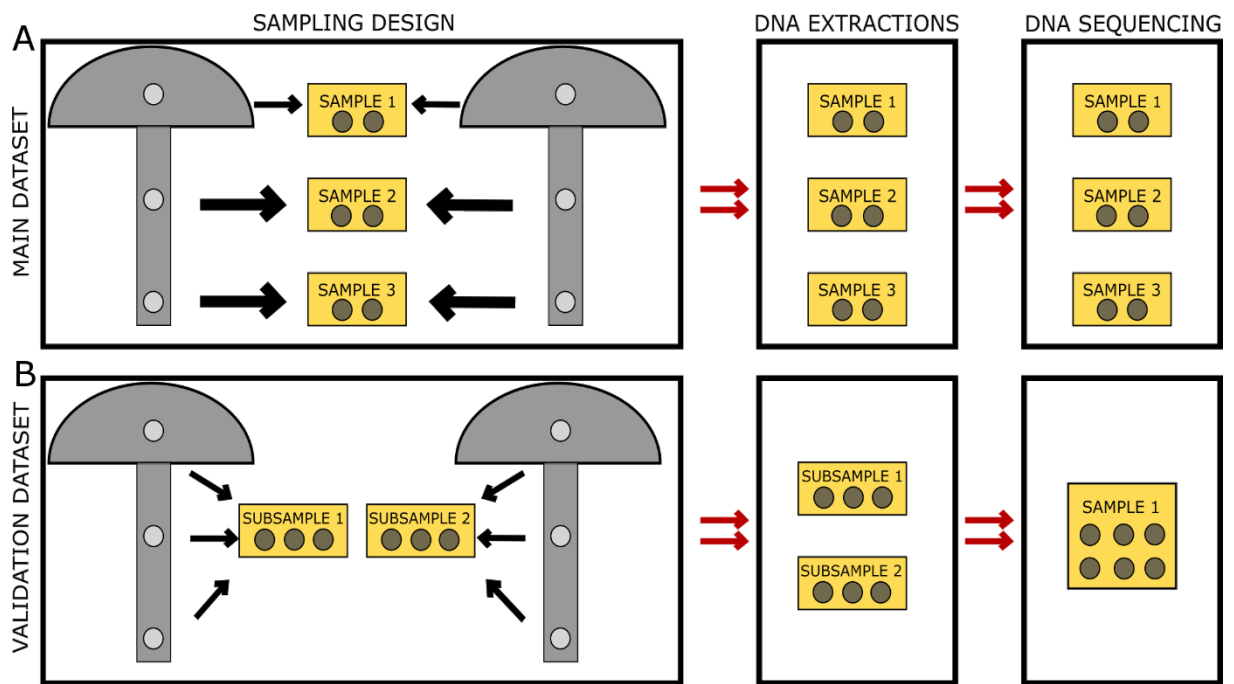


Figure S2. The schematic illustration of the fruitbody sampling design for the main dataset (A) and in the validation dataset (B). The fruitbody pieces were collected from two halves and different parts of one fruitbody and handling of the pieces in the DNA extraction and sequencing steps.

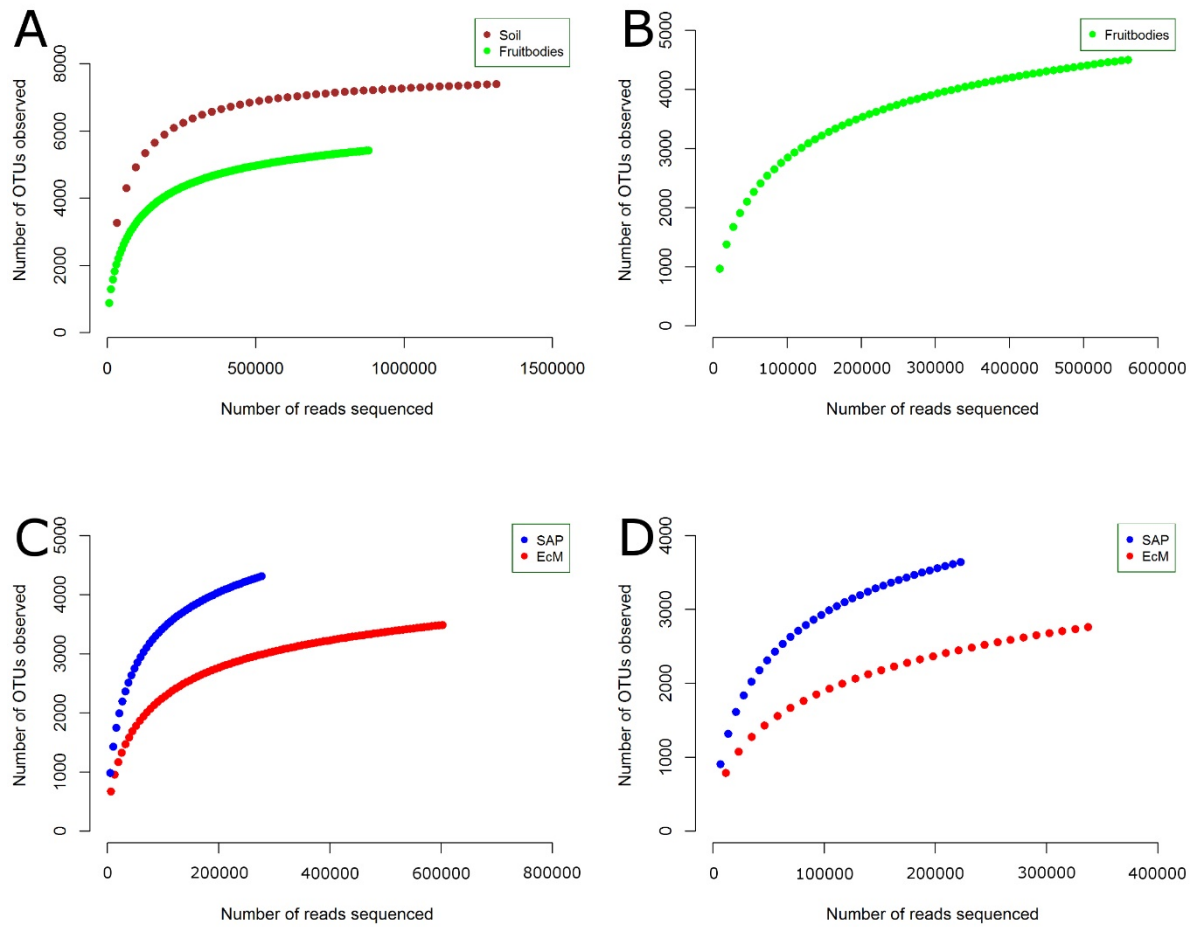


Figure S3. Rarefaction curves for fruitbody and soil samples from main dataset (**A**) and for fruitbody samples from validation dataset (**B**) as well as for ectomycorrhizal (EcM) and saprotrophic (SAP) fruitbody samples from main dataset (**C**) and from validation dataset (**D**). Each symbol represents one of the three fruitbody parts in the main dataset (**A**, **C**) and the whole fruitbody in the validation dataset (**B**, **D**).

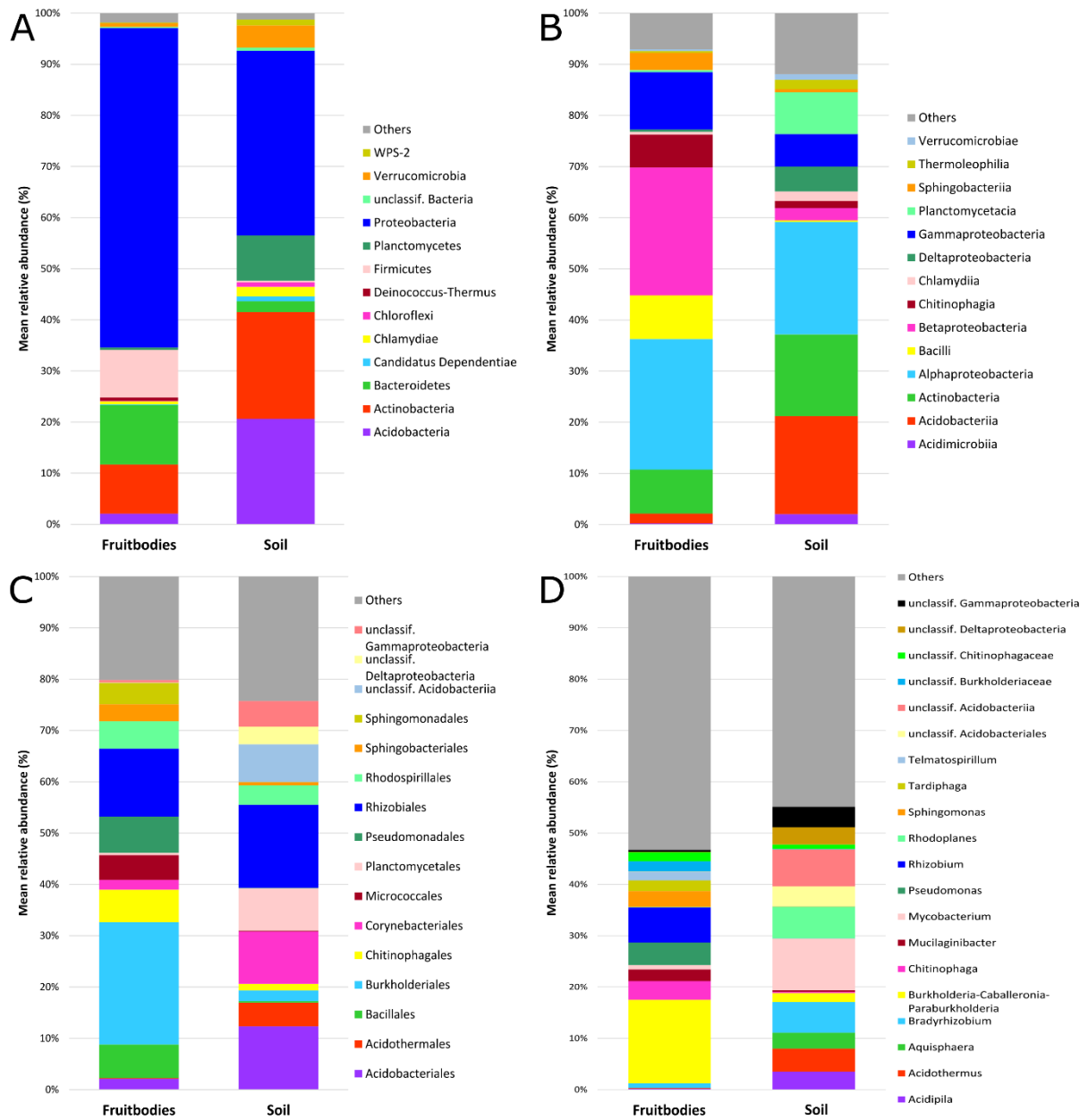


Figure S4. The mean relative abundance (%) of ten most numerous bacterial phyla (A), classes (B), orders (C) and genera (D) in fruitbodies and in soil based on HTS read numbers normalized by the total number of reads per each sample.

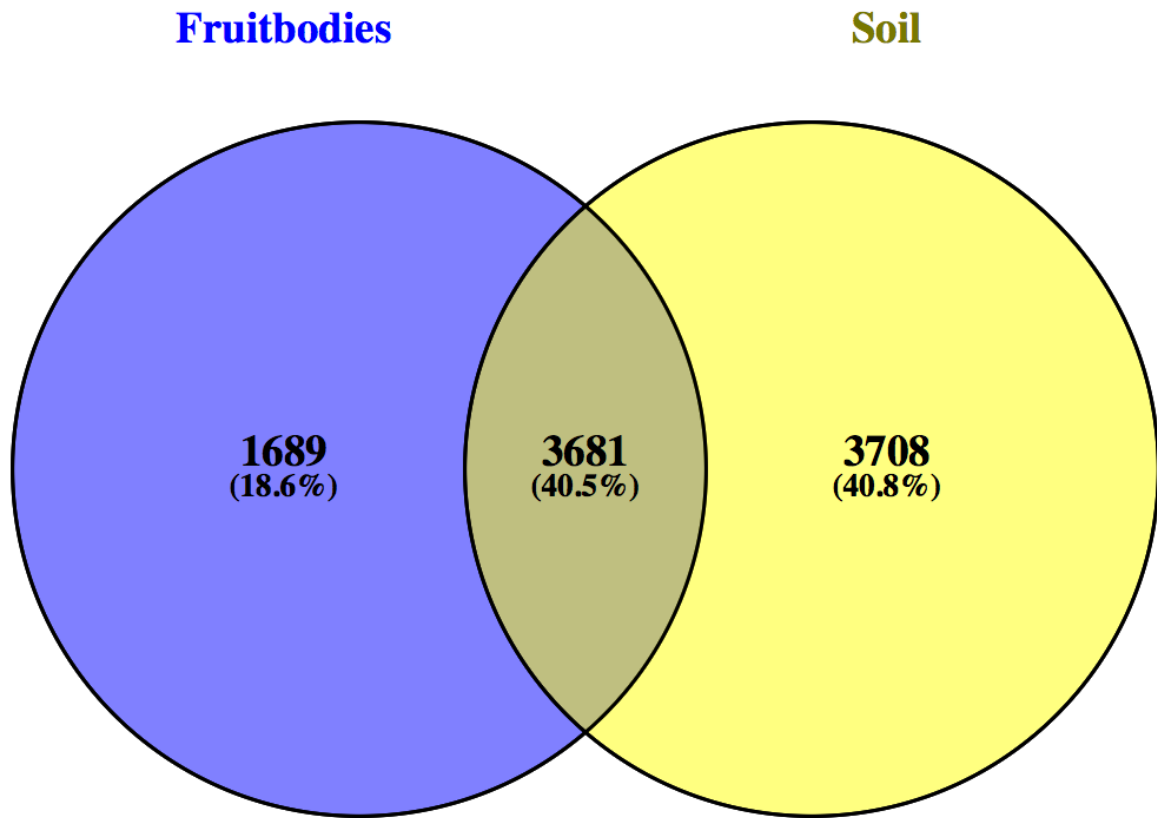


Figure S5. The numbers of unique and shared OTUs in the fruitbodies and in the surrounding soil.

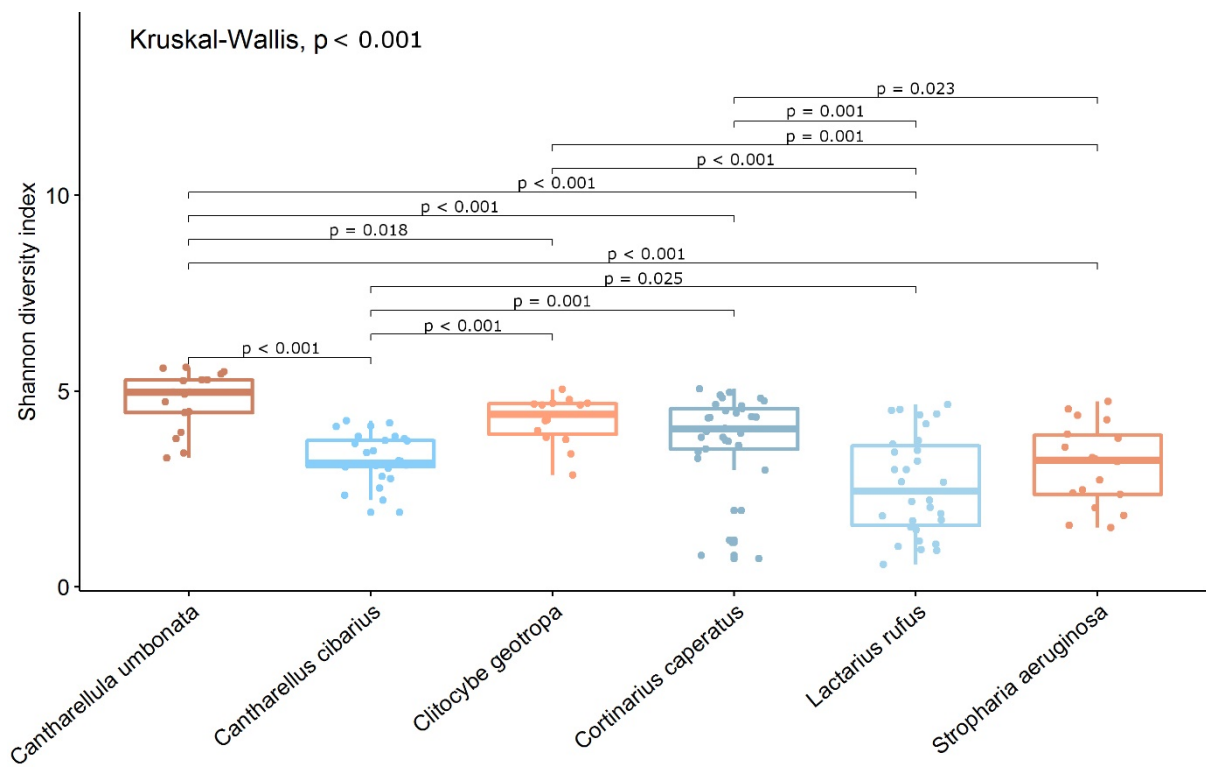


Figure S6. Boxplot showing differences in the diversity of the microbial communities in six studied fungal species based on Shannon indices. Significant pairwise differences ($p \leq 0.05$) are represented based on Wilcoxon test results. Brown tones indicate saprotrophic species and blue tones indicate ectomycorrhizal species. Each dot represents one of the three fruitbody parts.

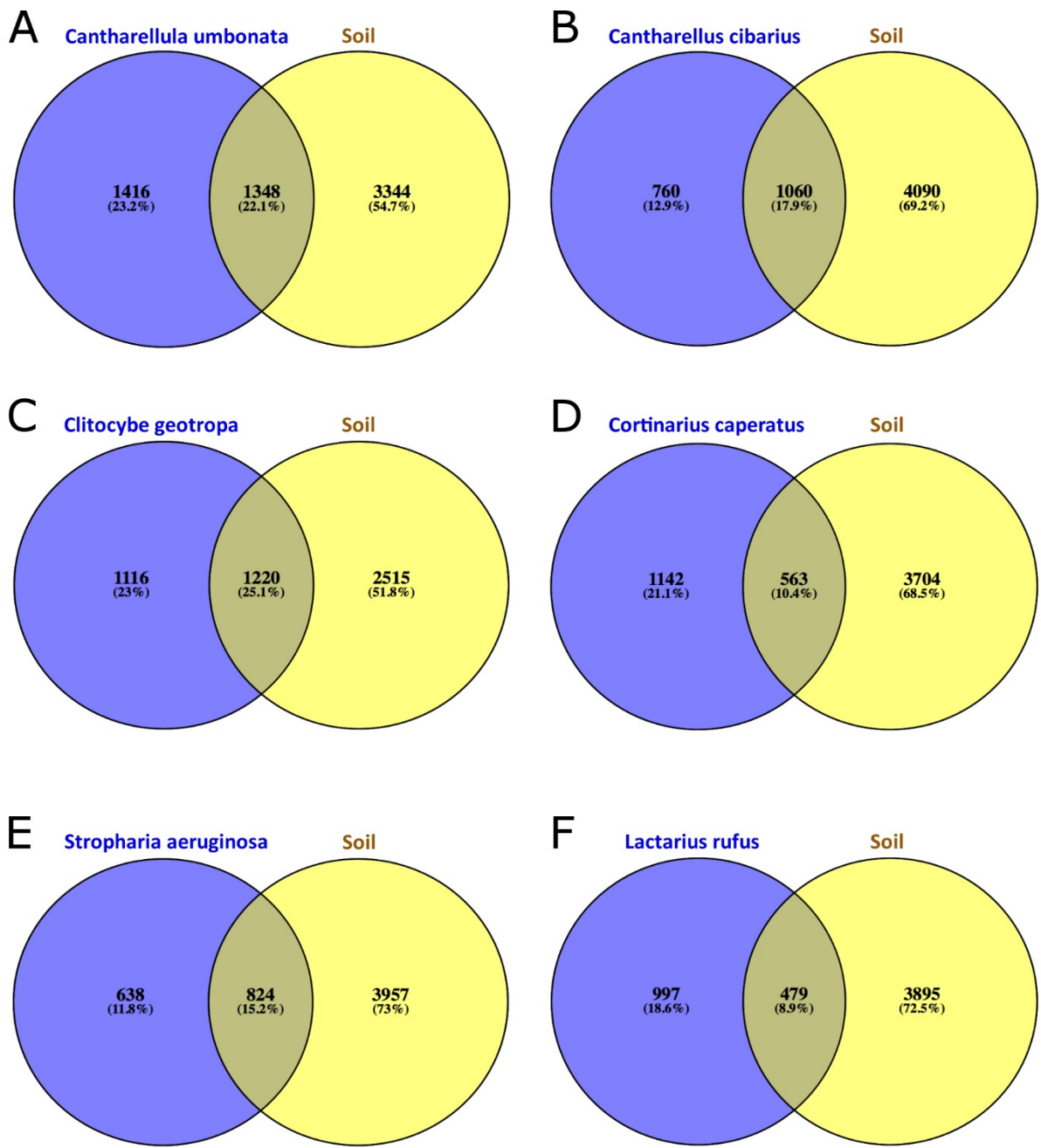


Figure S7. The numbers of unique and shared OTUs in three saprotrophic (A,C,E) and three ectomycorrhizal species (B, D, F) and in the corresponding soil samples.

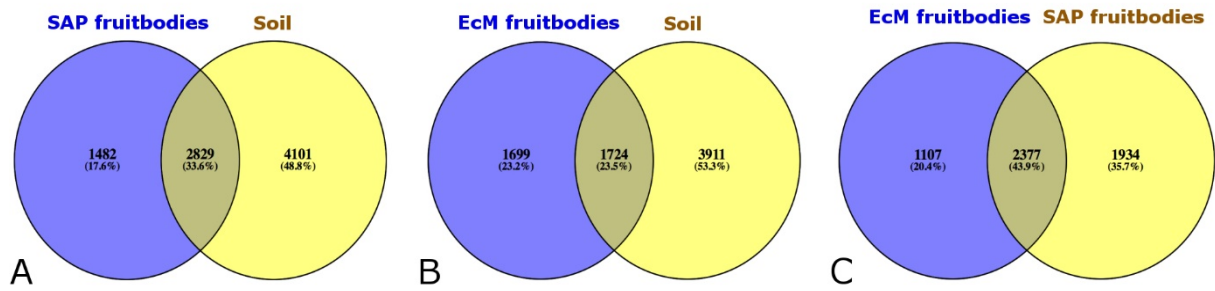


Figure S8. The numbers of unique and shared bacterial OTUs in the fruitbodies of saprotrophic (SAP) fungi and their surrounding soil (A), ectomycorrhizal (EcM) fungi and their surrounding soil (B) as well as EcM and SAP fungi (C).

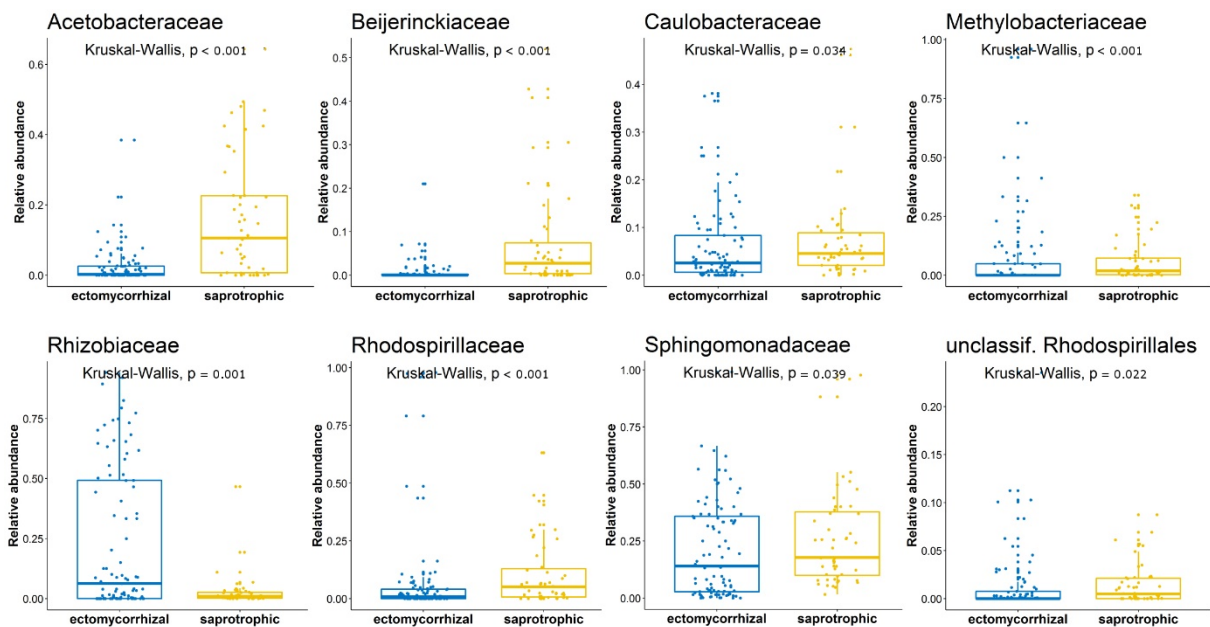


Figure S9. Significant differences of the relative abundances of ten most numerous fruitbody-inhabiting bacterial families among the class Alphaproteobacteria between ectomycorrhizal and saprotrophic fungi based on Kruskal-Wallis test. The HTS read numbers were normalized by the total number reads per each sample. Each dot represents one of the three fruitbody parts.

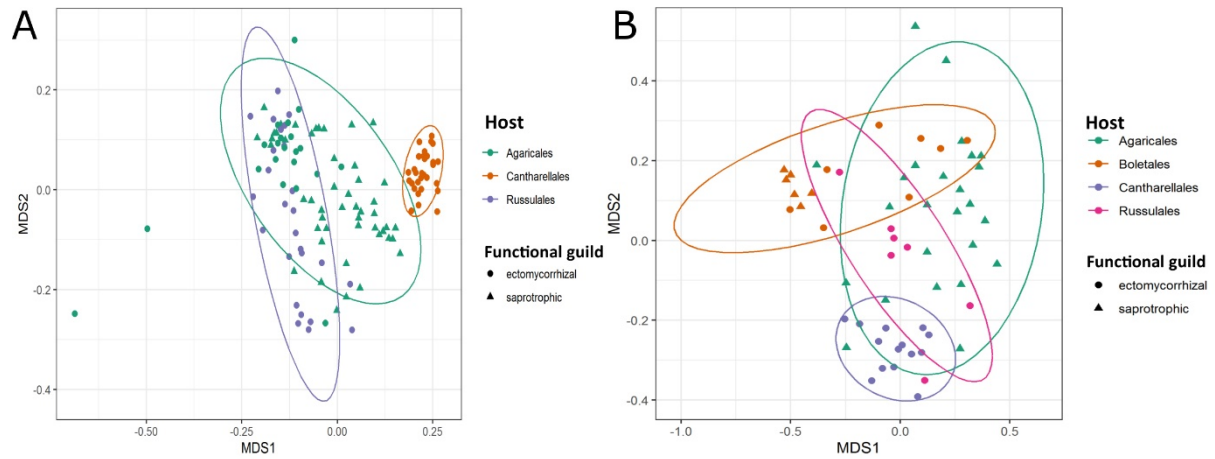


Figure S10. Non-metric multidimensional scaling (NMDS) ordination illustrating compositional differences in bacterial communities across different host fungal orders and functional guilds in the main dataset **(A)** and in the validation dataset **(B)**. The Bray-Curtis dissimilarity matrix is calculated based on rarified and Hellinger transformed OTU matrix. Each dot represents one of the three fruitbody parts and the samples were rarified to ≤ 2000 reads in the main dataset **(A)** and each dot represents the whole fruitbody and the samples were rarified to ≤ 5000 reads in the validation dataset **(B)**. Samples containing less than 1000 reads were removed. The functional guild effect is involved in NMDS, because PERMANOVA results revealed its significant impact (**A**: $p \leq 0.001$; **B**: $p = 0.014$) on the bacterial community composition in fruitbodies.

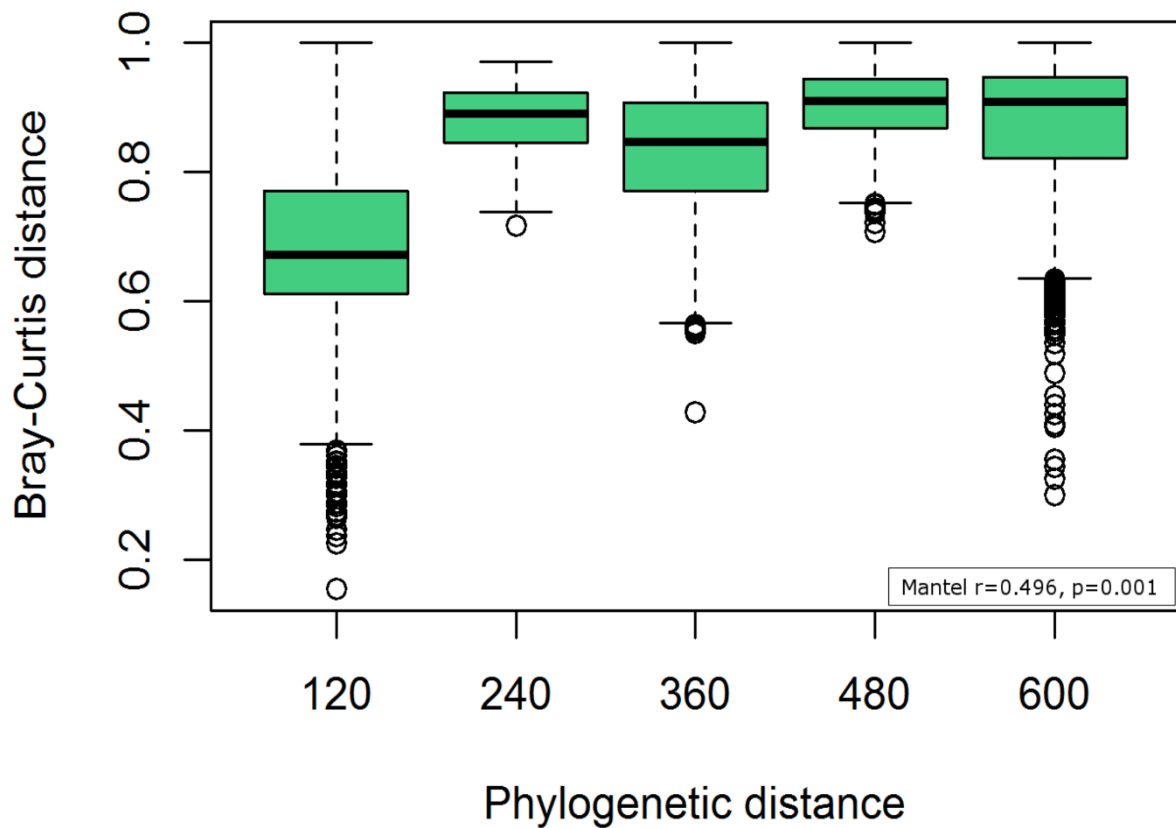


Figure S11. The relationship of dissimilarities among the bacterial community composition in the fruitbodies of six fungal species with the phylogenetic distance of the host fungi. The phylogenetic distance has been calculated based on the taxonomy tree, created by the perl script taxonomy_to_tree.pl following Tedersoo et al. (2018). The phylogenetic distance is converted to the random numerical units on x-axis. Six species ended up in five phylogenetic distance baskets, because two of them (*Cantharellula umbonata* and *Clitocybe geotropa*) were taxonomically close, belonging both into the family Tricholomataceae.

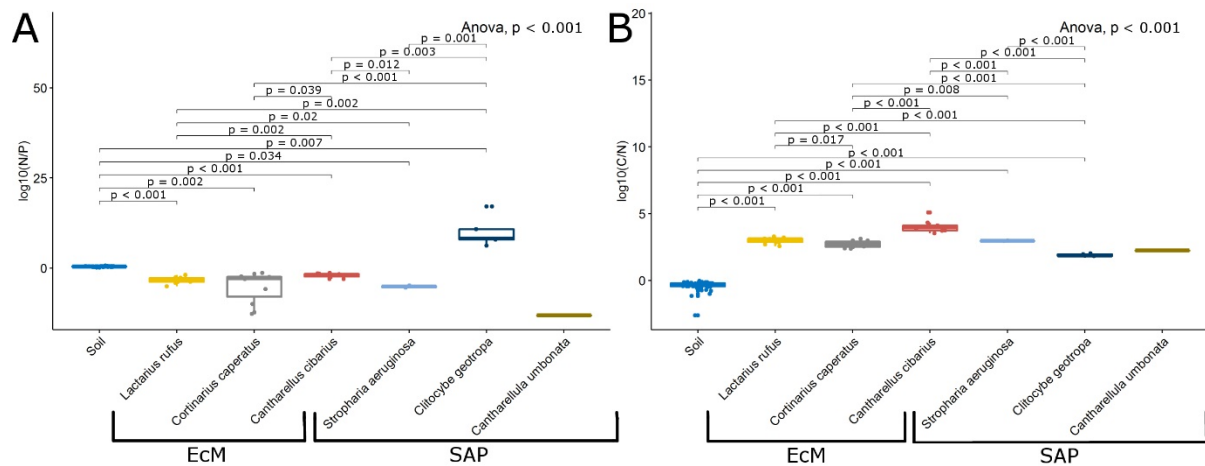


Figure S12. Boxplots illustrating the variation of N/P ratio (A) and C/N ratio (B) among fungal species and soil; t-test results indicated the pairwise significant differences among fungal species and soil and ANOVA results showed the significance of the variation of these characteristics among fungi and soil in general. The N, P and C values were log-transformed. Each dot represents the whole fruitbody or a soil sample. Species *Cantharellula umbonata* is presented as one replicate (all their individual fruitbodies were analyzed together as one sample) and was not involved into the statistical analyses (t-test, ANOVA).

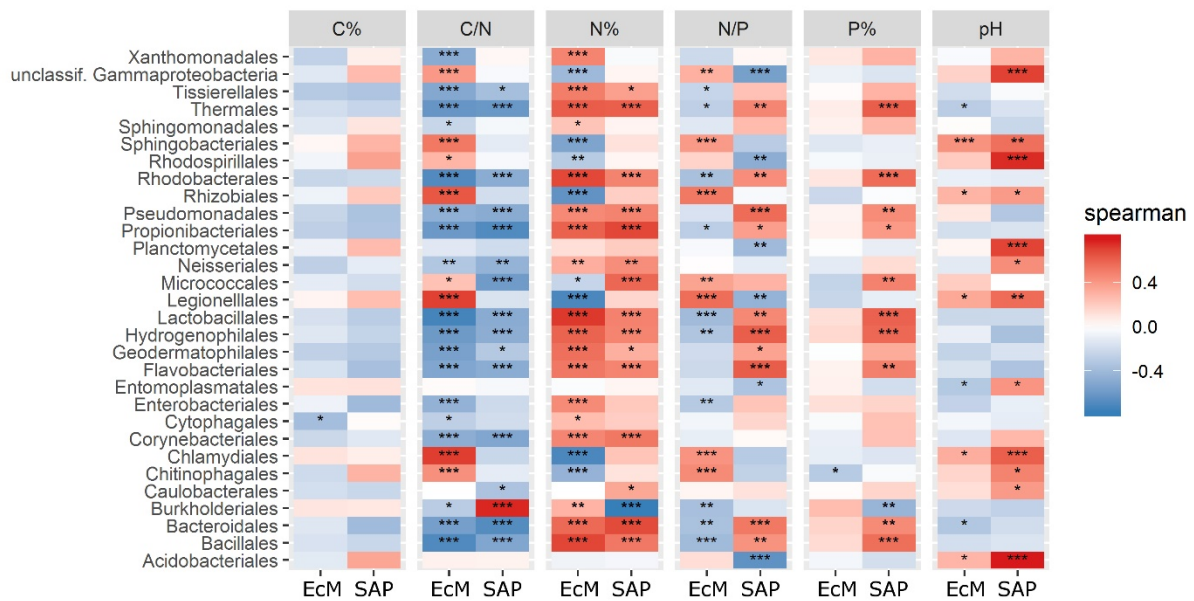


Figure S13. The Spearman correlations between the abundance of 30 most numerous bacterial orders and chemical properties of fruitbodies of ectomycorrhizal (EcM) and saprotrophic (SAP) fungi in the main dataset. ***: P-value ≤ 0.001 , **: P-value ≤ 0.01 , *: P-value ≤ 0.05

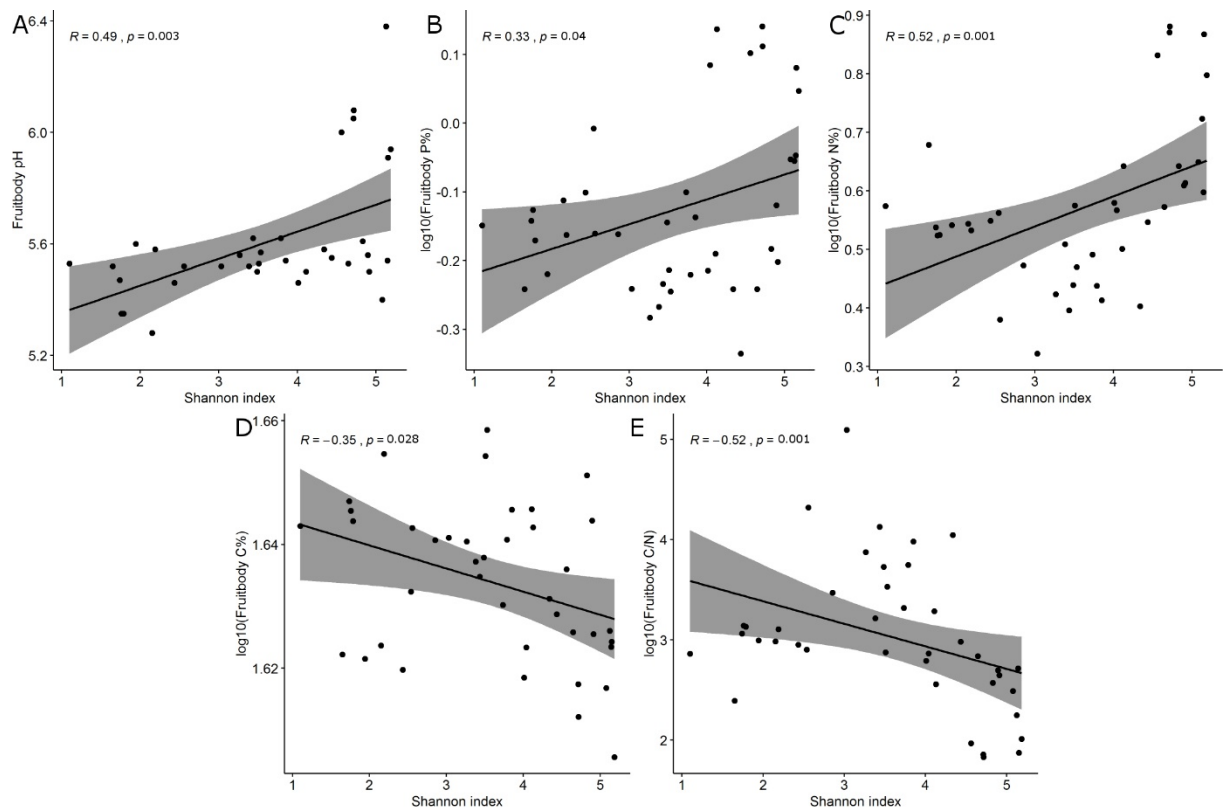


Figure S14. The scatterplots illustrating the significant correlations ($p \leq 0.05$) between the fruitbody pH (A), P% (B), N% (C), C% (D) as well as C:N ratio (E) and the bacterial diversity metrics in fruitbodies (Shannon indices). The indicators have been calculated using the Spearman's correlation test and the C, N and P values were log-transformed. Each symbol represents a fruitbody.

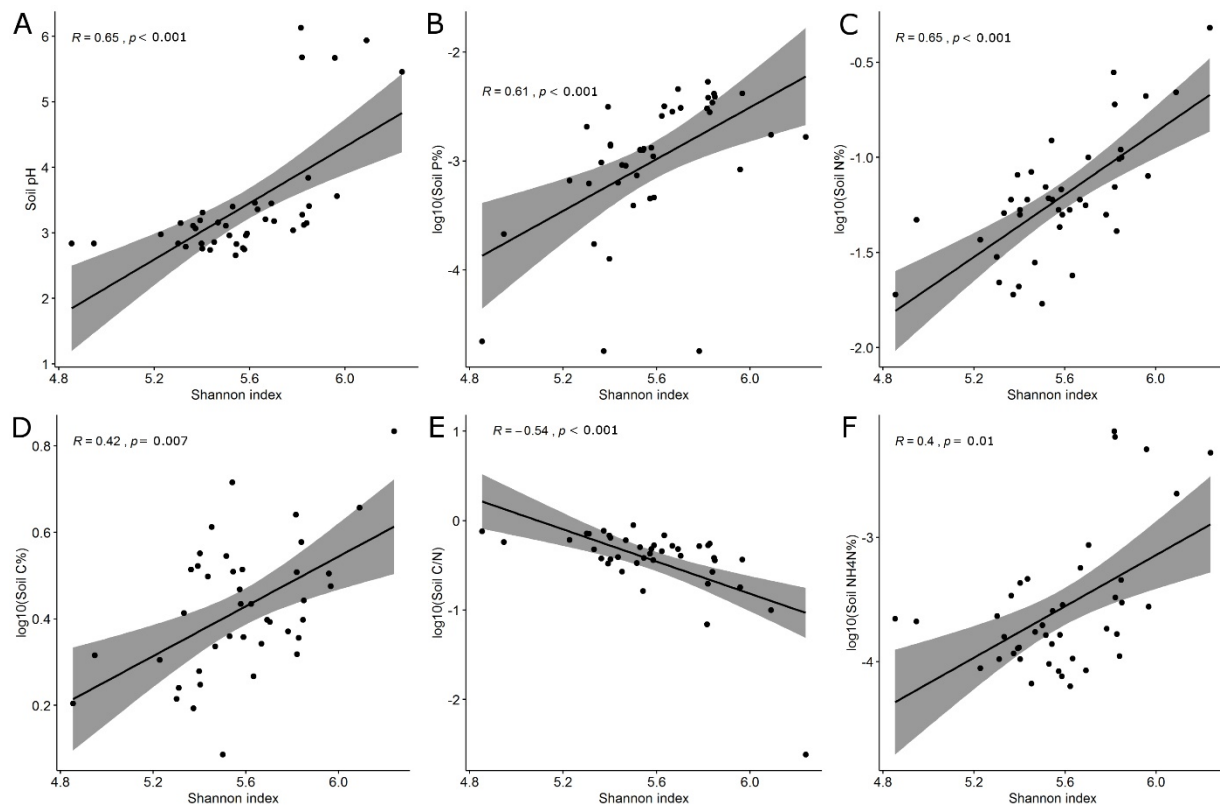


Figure S15. The scatterplots illustrating the significant correlations ($p \leq 0.05$) between the soil pH (A), P% (B), N% (C), C% (D), C:N ratio (E) as well as $\text{NH}_4\text{N}\%$ (F) and the bacterial diversity metrics in soil (Shannon indices). The indicators have been calculated using the Spearman's correlation test and the C, N, P and NH_4N values were log-transformed. Each dot represents a soil sample.